



Analysis of the Phospholipid Profile of Metaphase II Mouse Oocytes Undergoing Vitrification

Jaehun Jung^{1,3*}, Hyejin Shin^{2*}, Soyoung Bang², Hyuck Jun Mok³, Chang Suk Suh⁴, Kwang Pyo Kim^{3*}, Hyunjung Jade Lim^{2*}

1 Department of Pharmacology, Konkuk University School of Medicine, Seoul, Korea, **2** Department of Biomedical Science & Technology, Institute of Biomedical Science & Technology, Konkuk University, Seoul, Korea, **3** Department of Applied Chemistry, College of Applied Science, Kyung Hee University, Yongin, Gyeonggi-do, Korea, **4** Department of Obstetrics and Gynecology, Seoul National University Bundang Hospital, Seongnam, Gyeonggi-do, Korea

Abstract

Oocyte freezing confers thermal and chemical stress upon the oolemma and various other intracellular structures due to the formation of ice crystals. The lipid profiles of oocytes and embryos are closely associated with both, the degrees of their membrane fluidity, as well as the degree of chilling and freezing injuries that may occur during cryopreservation. In spite of the importance of lipids in the process of cryopreservation, the phospholipid status in oocytes and embryos before and after freezing has not been investigated. In this study, we employed mass spectrometric analysis to examine if vitrification has an effect on the phospholipid profiles of mouse oocytes. Freshly prepared metaphase II mouse oocytes were vitrified using copper grids and stored in liquid nitrogen for 2 weeks. Fresh and vitrified-warmed oocytes were subjected to phospholipid extraction procedure. Mass spectrometric analyses revealed that multiple species of phospholipids are reduced in vitrified-warmed oocytes. LIFT analyses identified 31 underexpressed and 5 overexpressed phospholipids in vitrified mouse oocytes. The intensities of phosphatidylinositol (PI) {18:2/16:0} [M-H]⁻ and phosphatidylglycerol (PG) {14:0/18:2} [M-H]⁻ were decreased the most with fold changes of 30.5 and 19.1 in negative ion mode, respectively. Several sphingomyelins (SM) including SM {d38:3} [M+H]⁺ and SM {d34:0} [M+K]⁺ were decreased significantly in positive ion mode. Overall, the declining trend of multiple phospholipids demonstrates that vitrification has a marked effect on phospholipid profiles of oocytes. These results show that the identified phospholipids can be used as potential biomarkers of oocyte undergoing vitrification and will allow for the development of strategies to preserve phospholipids during oocyte cryopreservation.

Citation: Jung J, Shin H, Bang S, Mok HJ, Suh CS, et al. (2014) Analysis of the Phospholipid Profile of Metaphase II Mouse Oocytes Undergoing Vitrification. PLoS ONE 9(7): e102620. doi:10.1371/journal.pone.0102620

Editor: Xiaoming He, The Ohio State University, United States of America

Received: April 18, 2014; **Accepted:** June 19, 2014; **Published:** July 17, 2014

Copyright: © 2014 Jung et al. This is an open-access article distributed under the terms of the Creative Commons Attribution License, which permits unrestricted use, distribution, and reproduction in any medium, provided the original author and source are credited.

Data Availability: The authors confirm that all data underlying the findings are fully available without restriction. All relevant data are within the paper and its Supporting Information files.

Funding: This study was supported by a grant from the Korea Health Technology R&D Project, Ministry of Health & Welfare, Republic of Korea (H12C0055, <https://www.htdream.kr/>). The funders had no role in study design, data collection and analysis, decision to publish, or preparation of the manuscript.

Competing Interests: Corresponding author Hyunjung Jade Lim is a PLOS ONE Editorial Board member. This does not alter the authors' adherence to PLOS ONE's editorial policies and criteria.

* Email: kimkp@khu.ac.kr (KPK); hlim@konkuk.ac.kr (HJL)

† These authors contributed equally to this work.

Introduction

The management of female fertility through the cryopreservation of oocytes or ovarian tissue has many advantages. Cryopreservation can be used to keep extra oocytes after an in vitro fertilization (IVF) cycle and to preserve the oocytes of cancer patients or women who wish to store their oocytes for social reasons [1,2]. Based on the clinical outcomes of several studies, the most recent guidelines on mature oocyte cryopreservation recommend that oocyte vitrification and warming should no longer be considered an experimental practice based on clinical outcomes of several studies [3]. Thus, the general need for cryopreservation of oocyte or ovarian tissue is expected to continue to increase. In this context, it is necessary to fine-tune current cryopreservation techniques by using novel biochemical and molecular parameters. Two basic methods have been established for oocyte cryopreservation, slow-freezing and vitrifi-

cation [1]. For human oocytes, both of these methods are used in IVF clinics world-wide [3].

Oocyte freezing causes thermal and chemical stress in the oolemma and various other intracellular structures due to the formation of ice crystals. Permeating cryoprotectants (CPs), such as dimethyl sulfoxide (DMSO), ethylene glycol (EG), and propylene glycol (PEG), are generally used in combination with non-permeating sugar-type CPs in the vitrification solution to minimize such stresses [4]. Lipids are fundamental macromolecules in cells, constituting the membranes of various organelles and the plasma membrane [5]. They are also directly involved in signal transduction in the form of lipid mediators including phosphatidylinositols, phosphoinositides, sphingolipids, and eicosanoids [6]. Lipids also give rise to numerous types of small vesicles within cells that are involved in protein transport, autophagy, protein degradation, and other subcellular processes [5]. Membrane lipids, composed mainly of phospholipids, glycolipids, and

cholesterol, undergo a lipid phase transition (LPT) during chilling [7]. Membrane fluidity is tightly correlated with the composition of membrane lipids, a connection that is reflected in the difference in the LPT temperatures of distinct membranes [8]. There is a correlation between survival rates after cryopreservation and LPT temperatures. For example, human zygotes with low LPT temperature show a higher survival rate than oocytes with high LPT temperatures [7]. Chilling injury is known to compromise the membrane integrity of bovine oocytes [9]. Therefore, the lipid profiles of oocytes and embryos are closely associated with the degree of chilling and freezing injuries incurred during cryopreservation [7]. Despite the importance of lipids during cryopreservation, the status of phospholipids in oocytes and embryos before and after freezing has not been investigated.

Mass spectrometry is an integral technique used in lipidomics, a systemic approach to elucidate the lipid levels and composition in cells under various physiological and pathological conditions [10,11]. Lipid composition in oocytes and preimplantation embryos has been examined in mice and other species [12–15]; however, there is no data on whether the composition of phospholipids within these systems is affected by the cryopreservation process. In various disciplines, the results obtained using matrix-assisted laser desorption/ionization time-of-flight mass spectrometry (MALDI-TOF MS) have produced better diagnostic efficacy than other established diagnostic tools. MALDI-TOF MS is a fast, sensitive, and highly reliable method to analyze changes in macromolecules in small quantities of biological material. In this study, we analyzed the phospholipid profile in mouse oocytes prior to and following vitrification by using MALDI-TOF MS. Our purpose in this study was to determine whether the vitrification-warming process affected the phospholipid profile in oocytes. To the best of our knowledge, we are the first to demonstrate that specific phospholipids are reduced or increased in mouse oocytes after cryopreservation and that the mass peaks of phospholipids are potential biomarkers of oocyte undergoing vitrification.

Results

Visualization of fatty acids and plasma membrane in mouse oocytes

To obtain general idea if vitrification affect the status of lipid-enriched subcellular structures in mouse MII oocytes is affected by vitrification, we stained them with two vital dyes. BODIPY 500/510, a fluorescent fatty acid analog, and CellMask deep red stain labeled intracellular fatty acids and plasma membranes, respectively. As shown in Fig. 1B, fresh mouse MII oocytes possess numerous small lipid-containing vesicular structures (green) uniformly distributed throughout the ooplasm. In contrast, BODIPY-labeled structures tended to be larger and more condensed in solution-treated and vitrified-warmed oocytes. CellMask uniformly stained the periphery of fresh oocytes. In contrast, this staining pattern was less uniform in solution-treated and vitrified-warmed oocytes (Fig. 1). Taken together, these data indicate that CP-containing solutions cause an immediate osmotic shock and that lipid-containing subcellular structures and plasma membrane rapidly respond to this osmotic stress. Thus, this result provides a clue that vitrification process may alter various lipid-containing subcellular structures and phospholipid components of plasma membrane.

Phospholipid analyses of vitrified-warmed oocytes

To this end, we sought to investigate if quantifiable changes in lipid profiles occur in mouse oocytes after vitrification. Because lipid composition affects LPT upon chilling and freezing [8], it is

important to investigate vitrification-associated changes in oocyte phospholipid composition. Thus, we analyzed phospholipid profiles of mouse oocytes before and after vitrification using MALDI-MS. A group of oocytes were treated only with vitrification and warming solutions was included as control (Fig. 1A). A schematic diagram of the procedure is shown in Fig. 1A. To distinguish background peaks generated by the matrix, pure matrix profiles of both the binary and 9-aminoacridine matrices were determined (Fig. S1).

We compared representative MALDI spectra obtained for the phospholipid extracts of fresh and vitrified oocytes in positive ion mode (Fig. 2A) and negative ion mode (Fig. 2B). As shown in Fig. 2A, the majority of phospholipid peaks, including major mass peaks m/z 760.6 and m/z 782.6, were reduced in the vitrification group. From two biological replicates (total 200 oocytes in each group), spectra were obtained from 20 technical replicates and 15 technical replicates in positive and negative ion modes, respectively, with reproducible results. The spectra of vitrified oocytes, showed an overall decreasing trend for the majority of mass peaks. Thus, the phospholipid profiling of oocytes with MALDI-MS is reproducible and comparable in terms of m/z values and signal intensity.

We next performed PCA using ClinProTools 2.2 software (Fig. 3) [16]. Total MALDI-MS datasets acquired in positive and negative ionization modes were analyzed. A number of m/z values showed significant distribution changes in oocyte phospholipid extracts. As shown in Fig. 3, fresh and vitrified oocytes were separated by a large gap in PCA plots. The MALDI spectra of phospholipids can separate fresh and vitrified oocytes with a 95% confidence interval. To determine whether CP-induced osmotic shock affects the phospholipid profiles of oocytes, we examined PCA plots of solution-treated oocytes. As shown in Fig. S2, the fresh and solution-treated oocyte plots were closely situated, but were separate from that of vitrified oocytes. Representative spectra from fresh and solution-treated oocytes were also similar (Fig. S2). Thus, the vitrification process significantly changed the phospholipid profile of oocytes; however, the vitrification and warming solutions themselves did not have noticeable effect on mass spectra (Fig. S2). While the vitrification solution-associated osmotic changes may temporarily alter the organization of fatty acid-enriched subcellular structures (Fig. 1B), it does not appear to cause quantifiable fluctuations in the phospholipid pool. Fig. 4 shows representative fragmentation spectra in positive and negative ionization modes. The fragmentation spectrum of m/z 782.6; {PC 34:1} [M+Na]⁺ showed peaks corresponding to specific choline head groups containing phosphate (m/z 184), sodium adducted phosphate (m/z 147), and other distinct peaks corresponding to phospholipids (Fig. 4A). Fig. 4B shows the fragmentation spectrum of m/z 861.6. The fragmentation peaks contained a phosphatidylinositol head group (m/z 241) and fatty acid chains. The other identified phospholipids were annotated using LIFT mode and their fragmentation spectra are shown in Fig. S3.

Hierarchical cluster analysis (Fig. 5) [17] of the acquired MALDI-MS spectra also clearly suggest that the average peak intensities extracted from each set are well separated and easily distinguishable between fresh and vitrified oocytes. Our data provide putative biomarker peaks for phospholipids that show vitrification-induced changes. These peaks were identified with confidence using direct in situ analysis by using MALDI LIFT MS (Table 1).

The MALDI-MS analysis of lipid extracts of fresh and vitrified oocytes showed 36 major peaks common to the two datasets. In vitrified oocytes, 19 and 5 mass peaks were significantly decreased

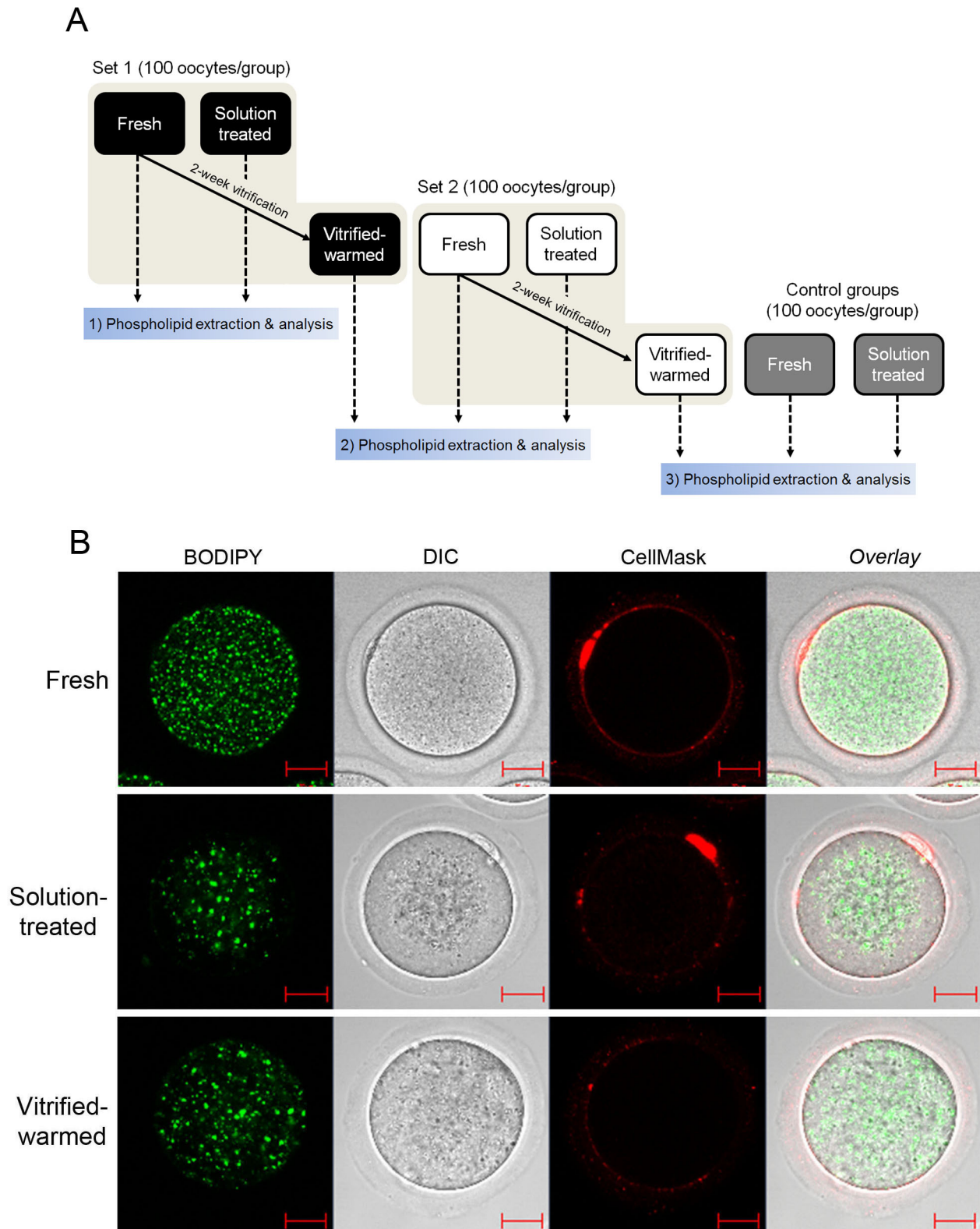


Figure 1. Experimental design and BODIPY/CellMask staining of mouse oocytes prior to and after vitrification. (A) A schematic diagram showing the experimental design and the three experimental groups. Two sets of vitrified-warmed oocytes with matching controls (represented as Set 1 and Set 2 in the diagram) were used. Since phospholipid extraction and subsequent analyses were performed on the day of oocyte preparation, the 2nd control groups were prepared on the day of thawing vitrified oocytes of the previous set. Another set of control oocytes were prepared when extracting phospholipids from vitrified-warmed oocytes of the 2nd set. This was added to ensure the quality of phospholipid extraction and analyses. Mass spectrometric analyses were performed in all groups shown. For statistical analysis, two full sets of data (shown in beige areas) excluding the last set of controls (shown in gray boxes) were included. (B) Fresh MII oocytes, solution-treated oocytes, and vitrified-warmed

oocytes (2-week vitrification) were stained with BODIPY 500/510 (10 $\mu\text{g/ml}$) and CellMask (2.5 $\mu\text{g/ml}$). Stained oocytes were washed with media and examined under a confocal microscope without fixation. BODIPY and CellMask are shown in green and red, respectively. The experiment was repeated more than three times with different pools of oocytes. Representative images are shown. Red scale bar, 20 μm .
doi:10.1371/journal.pone.0102620.g001

and increased in positive ion mode, respectively. In negative ion mode, 12 mass peaks had decreased (Table 1). Fig. 6C shows 9 phospholipids that were significantly reduced in vitrified oocytes (fold change >3 , $p < 0.01$). Phospholipids including phosphatidylcholines (PC), SM, PG, PI, and lysophosphatidylcholine (LPC) species were affected by vitrification. In positive ionization mode, SM {d38:3} [M+Na]⁺ and SM {d34:0} [M+K]⁺ showed the greatest reduction. In negative ionization mode, the intensities of PI {18:2/16:0} [M-H]⁻ and PG {14:0/18:2} [M-H]⁻ decreased the most with fold changes of 30.5 and 19.1, respectively. Overall, the downward trend of multiple phospho-

lipids demonstrates that vitrification can have a marked effect on lipid degradation.

Discussion

Endogenous lipids in oocytes and early preimplantation embryos are considered to be an energy substrate [18]. Lipid content varies greatly in mammalian oocytes. Mouse oocytes, for example, have a relatively lower fat content than domestic species [18,19]. Lipids play both structural and metabolic roles in mammalian oocytes. Therefore, the level of lipids within the

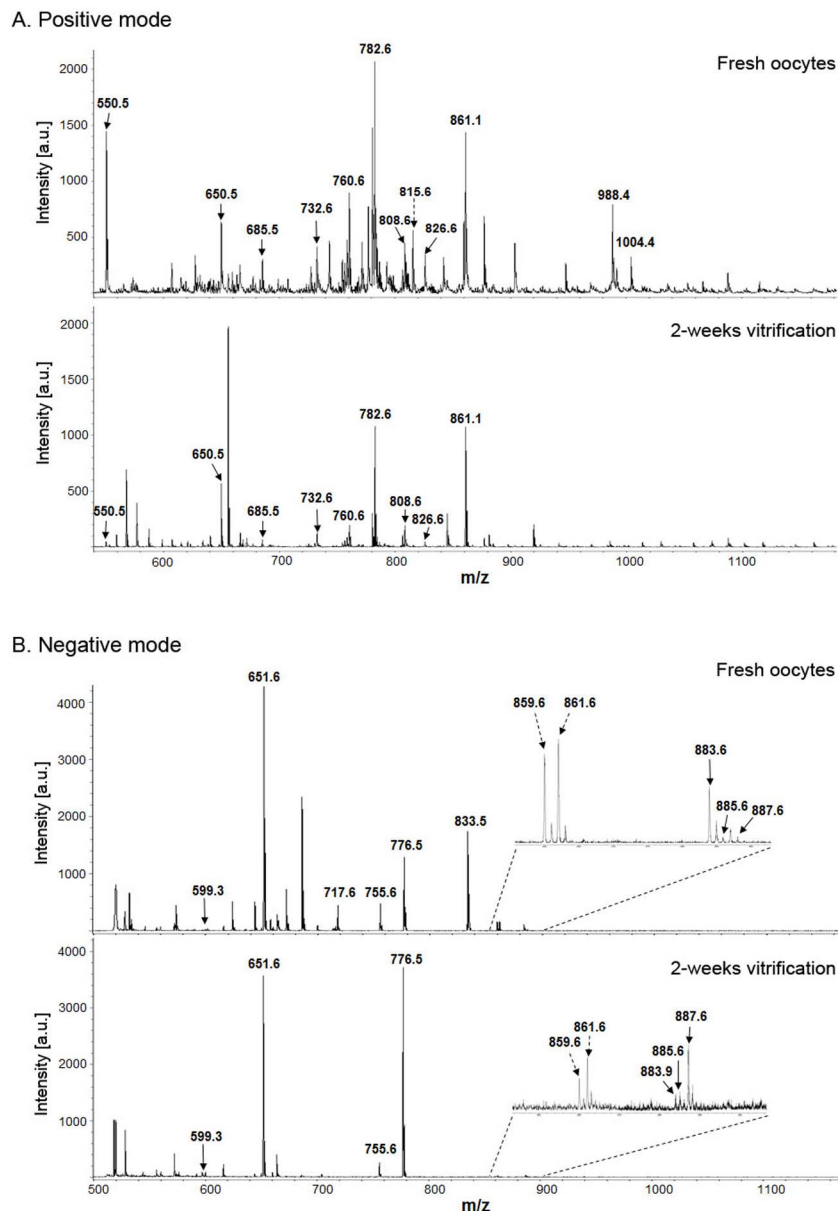


Figure 2. Representative mass spectra of lipids obtained from fresh and vitrified mouse oocytes in (A) positive ion mode and in (B) negative ion mode. m/z, mass-to-charge ratio; au, arbitrary unit.

doi:10.1371/journal.pone.0102620.g002

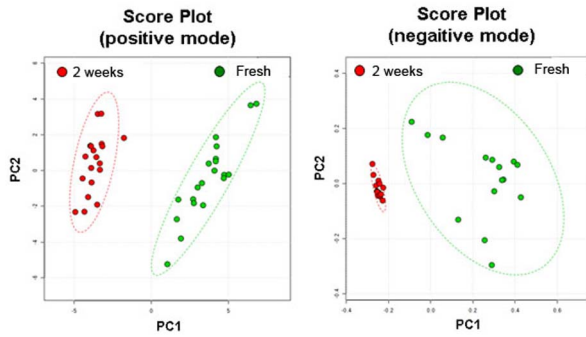


Figure 3. Principal component analysis plots for the phospholipid mass spectra. Fresh oocytes, green dots; 2-week vitrification, red dots.

doi:10.1371/journal.pone.0102620.g003

oocyte may reflect the degree of biochemical and physical stress it endures during cryopreservation. By using MALDI-MS, we demonstrated that phospholipids in oocytes undergo dynamic changes during cryostorage. Several major phospholipid species identified in the mass spectra (Fig. 2, Table 1) have been identified as predominant species in other mammalian oocytes [12,13,15],

confirming that the conditions of our analyses produced valid and reliable outputs. Of these major phospholipids, 31 phospholipids decreased and 5 increased in mouse oocytes in response to vitrification. Nine phospholipids showed a significant reduction in oocytes after vitrification (Fig. 6). In the mass spectra, major peaks including m/z 859.6, 903.7, 947.7, and 991.7 were identified as triglycerides. These peaks were also underexpressed in vitrified oocytes (data not shown). Therefore, our study was focused on the characterization of phospholipids, but we also confirmed that several species of triglycerides were reduced in vitrified oocytes. Whether these specific changes in phospholipid profile are more pronounced with longer storage periods (i.e., several months or years) shall make for interesting study. Further investigation is required to determine whether the method of slow freezing or the composition of CPs differentially affect phospholipid profiles.

In positive ionization mode, several sphingomyelins show large degree of reduction in vitrified oocytes when compared to fresh oocytes (Fig. 6). Several reports suggested that sphingomyelins exhibit high affinity towards cholesterol [20,21] and that their upregulation is associated with suppression of apoptosis [22]. Supplementation of sphingolipids has been proposed to protect mouse oocytes from undergoing apoptosis [23,24]. Whether the observed reduction in sphingomyelins in vitrified oocytes is linked

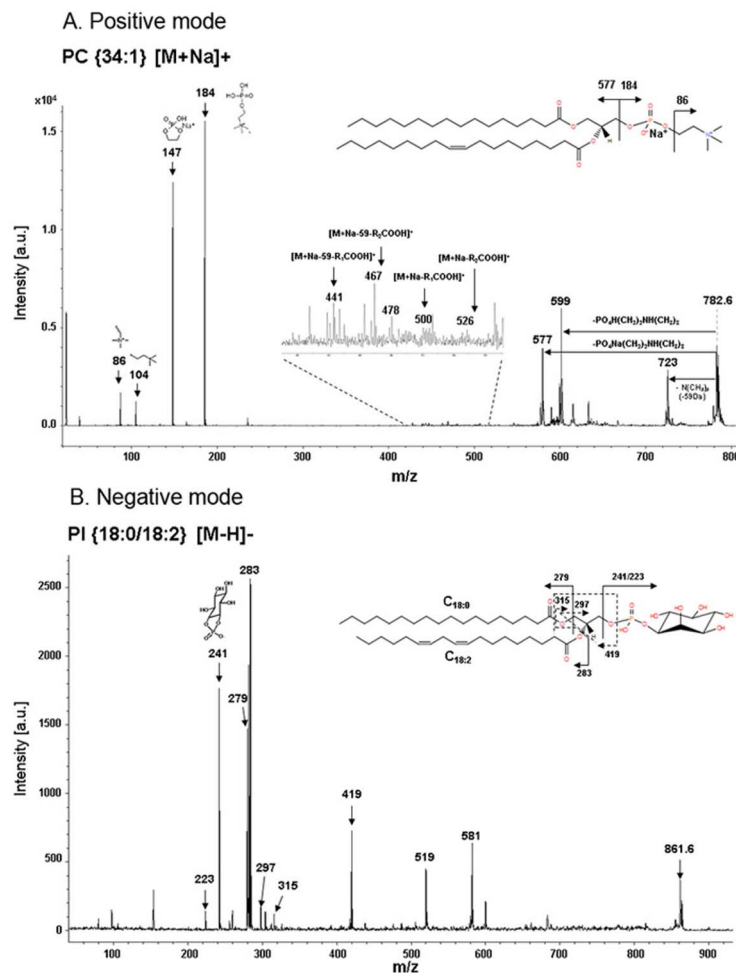


Figure 4. Fragmentation spectra of representative phospholipid species by using the LIFT technique. (A) m/z 782.6; PC {34:1} [M+Na]⁺ in positive ion mode and (B) m/z 861.6; PI {18:0/18:2} [M-H]⁻ in negative ion mode. Fragmentation spectra for other phospholipids are shown in Fig. S3.

doi:10.1371/journal.pone.0102620.g004

Table 1. Differentially expressed phospholipids between fresh oocytes and vitrified oocytes (2 weeks).

Underexpressed phospholipids in vitrified oocytes			Overexpressed phospholipids in vitrified oocytes				
<i>m/z</i>	<i>P</i> *	<i>Ratio</i> *	<i>Assignment</i>	<i>m/z</i>	<i>P</i>	<i>Ratio</i>	<i>Assignment</i>
<i>Positive mode</i>							
777.5	4.48E-23	10.44	SM {d38:3} [M+Na] ⁺	808.6	2.86E-01	0.96	PC {36:2} [M+Na] ⁺
743.6	1.53E-23	9.78	SM {d34:0} [M+K] ⁺	806.6	2.99E-04	0.86	PC {36:3} [M+Na] ⁺
815.6	1.12E-27	3.58	SM {d42:1} [M+H] ⁺	884.6	5.05E-07	0.82	PC {42:6} [M+Na] ⁺
550.5	4.72E-22	3.05	LPC {20:1} [M+H] ⁺	650.5	4.90E-10	0.69	PC {26:0} [M+H] ⁺
727.5	6.57E-23	2.42	SM {d34:0} [M+Na] ⁺	685.5	1.20E-13	0.61	SM {d30:1} [M+K] ⁺
795.6	1.84E-22	2.16	SM {d38:2} [M+K] ⁺				
798.6	4.16E-10	1.88	PC {34:1} [M+K] ⁺				
780.6	1.33E-14	1.66	PC {36:5} [M+H] ⁺				
754.6	1.29E-13	1.65	PC {34:4} [M+H] ⁺				
794.6	7.21E-15	1.63	PC {p-38:4} [M+H] ⁺				
826.6	1.95E-10	1.61	PC {38:7} [M+Na] ⁺				
758.6	6.28E-09	1.48	PC {34:2} [M+H] ⁺				
760.6	1.25E-06	1.42	PC {34:1} [M+H] ⁺				
786.6	2.33E-05	1.35	PC {36:2} [M+H] ⁺				
768.6	4.45E-07	1.25	PC {p-36:3} [M+H] ⁺				
756.6	3.05E-07	1.24	PC {34:3} [M+H] ⁺				
732.6	0.000019421	1.18	PC {32:1} [M+H] ⁺				
723.5	6.6907E-06	1.17	SM {d34:2} [M+Na] ⁺				
782.6	0.2259	1.04	PC {34:1} [M+Na] ⁺				
<i>Negative mode</i>							
833.6	5.93E-17	30.52	PI {18:2/16:0} [M-H] ⁻				
717.6	6.68E-11	19.17	PG {14:0/18:2} [M-H] ⁻				
699.5	2.54E-17	7.48	PA {18:2/18:0} [M-H] ⁻				
883.6	3.82E-09	4.38	PI {20:4/18:1} [M-H] ⁻				
859.6	1.32E-08	3.42	PI {18:2/18:1} [M-H] ⁻				
755.6	3.39E-11	2.88	PG {O-16:0/20:4} [M-H] ⁻				
861.6	6.85E-09	2.82	PI {18:0/18:2} [M-H] ⁻				
885.6	3.41E-05	1.91	PI {20:4/18:0} [M-H] ⁻				
677.7	5.27E-03	1.60	PG {p-16:0/14:0} [M-H] ⁻				

Table 1. Cont.

Underexpressed phospholipids in vitrified oocytes		Overexpressed phospholipids in vitrified oocytes	
<i>m/z</i>	<i>P</i> *	<i>Ratio</i> *	<i>Assignment</i>
<i>Positive mode</i>	<i>Positive mode</i>	<i>Ratio</i>	<i>Assignment</i>
599.3	1.59E-05	1.50	LPI [18:0] [M–H]–
776.6	6.22E-04	1.29	PE [p-20:0/20:5] [M–H]–
887.6	1.41E-01	1.18	PI {20:3/18:0} [M–H]–

**Ratio*, Fresh oocytes/2 weeks vitrified oocytes.
 **P*, *p* value.
 *PC, Phosphatidylcholines.
 *SM, Sphingomyelins.
 *LPC, Lysophosphatidylcholine.
 *PI, Phosphatidylinositol.
 *PG, Phosphatidylglycerol.
 *LPI, Lysophosphatidylinositol.
 *PE, Phosphatidylethanolamine.
 doi:10.1371/journal.pone.0102620.t001

PMSG (Sigma-Aldrich, St. Louis, MO, USA) and 7.5 IU hCG at a 48 h intervals. After 13–14 h after hCG injection, mice were sacrificed and oviducts were collected. Each mouse typically ovulated approximately 17–20 cumulus-oocyte complexes (COCs). COCs were collected by oviduct flushing 13–14 h post-hCG injection. Cumulus cells were removed by treating COCs with hyaluronidase (300 µg/ml) for 2 min. MII oocytes were collected, transferred to Quinn's Advantage medium with *N*-2-hydroxyethylpiperazine-*N'*-2-ethanesulfonic acid (HEPES, Cooper Surgical, Trumbull, CT, USA) containing 20% fetal bovine serum (FBS, Gibco, Life Technologies, Grand Island, NY, USA), and cultured at 37°C.

Vitrification and warming of mouse oocytes

Vitrification solutions contained EG (Sigma-Aldrich) and DMSO (Sigma-Aldrich) as cryoprotectants [34,35]. MII oocytes from 20–25 mice were pooled and pre-equilibrated in an equilibration solution (EQ) containing 7.5% EG, 7.5% DMSO, and 20% FBS in phosphate-buffered saline (PBS) [34]. Oocytes were then transferred to the vitrification solution containing 15% EG, 15% DMSO, 20% FBS, and 0.5 M sucrose in PBS (Fisher Scientific, St. Louis, MO, USA). After 20 s, 20 oocytes were loaded onto an electron microscopy copper grid (Ted Pella, Inc., Redding, CA, USA) and submerged in liquid nitrogen (LN₂). Vitrified oocytes were stored in LN₂ for 2 weeks. To thaw the oocytes, the grids were taken out of the LN₂ and directly put into thawing media (0.5 M sucrose and 20% FBS in PBS) for 2.5 min. Thawed oocytes (n = 100) were collected and sequentially incubated for 2.5 min in solutions containing decreasing concentrations of sucrose (0.25 M, 0.125 M, and 0 M). Finally, oocytes recovered for 1 h in Quinn's-HEPES media containing 20% FBS and incubated at 37°C in 5% CO₂. Oocytes without obvious morphological deformation or discoloration were selected and used for further analyses. Oocytes that survived the thawing process (~98%) were subjected to lipid extraction. In our routine laboratory procedures, vitrified-warmed mouse oocytes showed average of 62% fertilization rate and ~50% developmental rate to the blastocyst stage [36].

Fluorescence staining and confocal live imaging

BODIPY fatty acid 500/510 (D-3823) and CellMask Deep Red Plasma Membrane Stain (C10046) were purchased from Invitrogen (Carlsbad, CA, USA). BODIPY was dissolved in DMSO and diluted to 10 µg/ml in Quinn's-HEPES media (Cooper Surgical). CellMask was used at 2.5 µg/ml in media. MII oocytes were stained with the fluorescent dyes for 30 min, washed three times with media, and transferred to a glass-bottom confocal dish (SPL Life Sciences, Pocheon, Korea) [37,38]. Live images were captured using a Zeiss LSM710 confocal microscope (Zeiss, Germany) outfitted with a 40×C-Apochromat water immersion objective.

Reagents

HPLC-grade methanol, chloroform, and water were purchased from Burdick and Jackson (Muskegon, MI, USA). 2,5-dihydroxybenzoic acid (DHB), α-cyano-4-hydroxycinnamic acid (CHCA), 9-aminoacridine, and trifluoroacetic acid (TFA) were purchased from Sigma-Aldrich.

Phospholipid extraction

Phospholipids were extracted from MII oocytes (100 oocytes/group) by using the Bligh & Dyer method [39]. The following three oocyte groups were prepared: fresh MII oocytes, oocytes

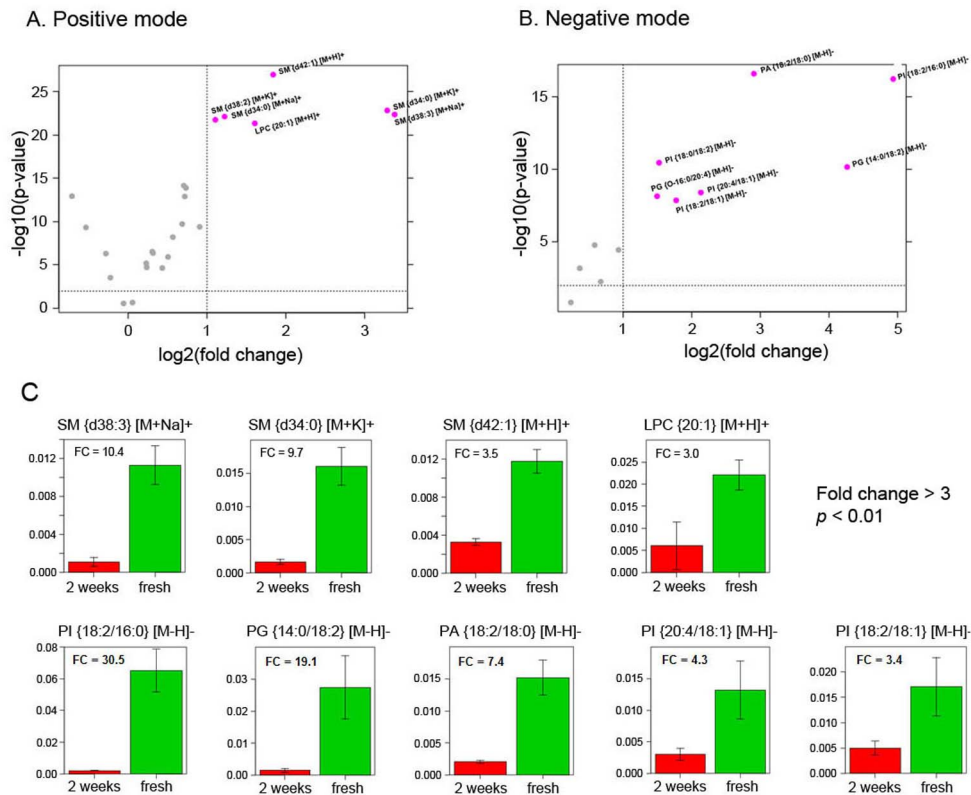


Figure 6. Relative intensities of differentially expressed phospholipids in fresh and vitrified oocytes measured by MALDI-TOF MS in (A) positive ion mode and in (B) negative ion mode. Red dots, phospholipid species with fold changes greater than 2 ($p < 0.01$). (C) Phospholipids that are significantly reduced after vitrification and warming. Fold changes greater than 3 are shown ($p < 0.01$). doi:10.1371/journal.pone.0102620.g006

treated with equilibration and vitrification solutions only (solution-treated), and oocytes vitrified for 2 weeks. As shown in Fig. 1A, two sets of vitrified-warmed oocytes with matching controls (represented as Set 1 and Set 2 in the diagram) were used. Since phospholipid extraction and subsequent analyses were all performed on the day of oocyte preparation, control groups were prepared on the day of thawing vitrified oocytes of the previous set. Therefore, another set of control oocytes were prepared when extracting phospholipids from vitrified-warmed oocytes of the 2nd set (Fig. 1A). For the extraction, oocytes were first rinsed with PBS several times to remove traces of culture media and then transferred into 3 ml of CHCl_3 :methanol (1:2, v/v) in 15 ml conical glass tubes. Each sample was vortexed vigorously for 1 min, sonicated for 10 min, and cooled on ice for 10 min. After adding 2.3 ml of CHCl_3 :water (1:1.3, v/v), the samples were vortexed vigorously and centrifuged at $2500 \times g$ for 10 min. The bottom organic phase containing the lipids was dried using a speed vacuum. All experiments were performed in duplicate.

Lipid MALDI-TOF MS analysis

A binary matrix solution was prepared by dissolving 3.5 mg each of DHB and CHCA into 1 ml of 70% methanol containing 0.1% TFA for the positive mode lipid MALDI-MS analysis [29,30,40,41]. 9-aminoacridine (5 mg/ml; dissolved in 6:4 isopropanol: acetonitrile, v/v) was used for the negative mode analysis [40,42]. The matrix suspensions (1.5 μl) were pipetted onto a stainless steel 384-well target plates (Bruker Daltonics, Billerica, MA, USA) and then dried in vacuum desiccator to equilibrate the

sample and matrix and reduce variability in the spectra. After sample spotting, each spot was analyzed directly by MS. MALDI MS analysis was performed using an Ultraflex III TOF/TOF mass spectrometer (Bruker Daltonics) equipped with a 200-Hz smart beam laser as the ionization source. The spectra were acquired using the following parameters: delay, 180 ns; ion source 1, 25 kV; ion source 2, 21.65 kV; and lens voltage, 9.2 kV. The MALDI-TOF was optimized for 550–1100 Da molecules and an average of 1000 shots/spot was acquired. Before each data acquisition, an external calibration was conducted using lipid-mixed calibration standards with mass-to-charge (m/z) ranges of 510–810 Da (positive ion mode) and 564–906 Da (negative ion mode). MALDI LIFT analysis was performed directly on the sample spot after the MALDI-MS analysis [43]. LIFT data were annotated using the lipid database, Lipidomics Gateway (www.lipidmaps.org).

Preprocessing of MALDI MS data

For each group, spectra were obtained 10 and 7 times in the positive and negative mode, respectively. All preprocessing steps were performed using a MALDIquant R package [44]. The intensity in single spectra were transformed to a square root scale for variance stabilization and smoothed using a moving average algorithm. The spectrum background was evaluated using the statistics-sensitive non-linear iterative peak-clipping (SNIP) algorithm and used for baseline correction. The intensities of multiple spectra were normalized using the probabilistic quotient normalization method. The features with signal-to-noise ratios higher

than 5 were detected as peaks. The peaks affiliated with the same mass were aligned by the statistical regression-based approach using the identification of landmark peaks and the estimation of a non-linear warping function. The raw data showing peak intensities are included in the Supporting Information (Tables S1–S3).

Statistical analysis of MALDI MS data

To compare multiple spectra from different samples, the following statistical analyses were performed using MetaboAnalyst 2.0 [45], a web-based software for quantitative data analysis. The input data for MetaboAnalyst analyses are given in the Supporting Information (Tables S4–S6). Half of the minimum positive value in the data replaced missing values in the data obtained from the preprocessing procedure. The intensity values of each peak across multiple spectra were mean-centered and divided by the standard deviation. Principal component analysis (PCA) was performed to show the relationship between variance in the data and differences among fresh and 2-week vitrified oocyte samples. The differentially expressed phospholipids were identified in volcano plots comparing fresh and vitrified oocytes by using the following criteria: (1) *P* values from the *t*-tests were less than 0.01 and (2) absolute fold changes were greater than 2. The raw data of volcano plots are given in the Supporting Information (Tables S7&S8). To show the relationship between samples and features, hierarchical clustering of the differentially expressed phospholipids was performed using Euclidean distances and Ward linkage. The Pearson's correlation coefficient of the features were calculated and clustered to identify correlating peaks.

Supporting Information

Figure S1 Pure matrix profiles of (A) binary matrix (positive ion mode) and (B) 9-aminoacridine (negative ion mode).
(DOC)

Figure S2 (A) Average mass spectra for lipids that are positive in fresh oocytes (red) and solution-treated oocytes (green). (B) A principal component analysis plot for phospholipid mass spectrum

of fresh oocytes (red), solution-treated control oocytes (green), and 2-weeks vitrified oocytes (blue).
(DOC)

Figure S3 Annotation of differentially expressed phospholipids (Table 1) by using the LIFT technique.
(PDF)

Table S1 MALDIquant output file: fresh vs vitrified oocytes in positive mode.
(XLSX)

Table S2 MALDIquant output file: fresh vs vitrified oocytes in negative mode.
(XLSX)

Table S3 MALDIquant output file: fresh vs media-treated vs vitrified oocytes in positive mode.
(XLSX)

Table S4 Metaboanalyst input file: fresh vs vitrified oocytes in positive mode.
(XLSX)

Table S5 Metaboanalyst input file: fresh vs vitrified oocytes in negative mode.
(XLSX)

Table S6 Metaboanalyst input file: fresh vs media-treated vs vitrified oocytes in positive mode.
(XLSX)

Table S7 Volcano plot data: fresh vs vitrified oocytes in positive mode.
(XLSX)

Table S8 Volcano plot data: fresh vs vitrified oocytes in negative mode.
(XLSX)

Author Contributions

Conceived and designed the experiments: KPK CSS HJL. Performed the experiments: JJ HS SB HJM. Analyzed the data: JJ HS KPK HJL. Contributed to the writing of the manuscript: JJ HS KPK HJL.

References

- Boldt J (2011) Current results with slow freezing and vitrification of the human oocyte. *Reprod Biomed Online* 23: 314–322. S1472-6483(10)00785-6 [pii];10.1016/j.rbmo.2010.11.019 [doi].
- Combelles CM, Chateau G (2012) The use of immature oocytes in the fertility preservation of cancer patients: current promises and challenges. *Int J Dev Biol* 56: 919–929. 120132cc [pii];10.1387/ijdb.120132cc [doi].
- The Practice Committees of the American Society for Reproductive Medicine and the Society for Assisted Reproductive Technology (2013) Mature oocyte cryopreservation: a guideline. *Fertil Steril* 99: 37–43. S0015-0282(12)02247-9 [pii];10.1016/j.fertnstert.2012.09.028 [doi].
- Saragusty J, Arav A (2011) Current progress in oocyte and embryo cryopreservation by slow freezing and vitrification. *Reproduction* 141: 1–19. REP-10-0236 [pii];10.1530/REP-10-0236 [doi].
- Schug ZT, Frezza C, Galbraith LC, Gottlieb E (2012) The music of lipids: how lipid composition orchestrates cellular behaviour. *Acta Oncol* 51: 301–310. 10.3109/0284186X.2011.643823 [doi].
- Di Paolo G, De Camilli P (2006) Phosphoinositides in cell regulation and membrane dynamics. *Nature* 443: 651–657. nature05185 [pii];10.1038/nature05185 [doi].
- Ghetler Y, Yavin S, Shalgi R, Arav A (2005) The effect of chilling on membrane lipid phase transition in human oocytes and zygotes. *Hum Reprod* 20: 3385–3389. dei236 [pii];10.1093/humrep/dei236 [doi].
- Arav A, Pearl M, Zeron Y (2000) Does membrane lipid profile explain chilling sensitivity and membrane lipid phase transition of spermatozoa and oocytes? *Cryo Letters* 21: 179–186.
- Arav A, Zeron Y, Leslie SB, Behboodi E, Anderson GB, et al. (1996) Phase transition temperature and chilling sensitivity of bovine oocytes. *Cryobiology* 33: 589–599. S0011-2240(96)90062-0 [pii];10.1006/cryo.1996.0062 [doi].
- Kim Y, Shanta SR, Zhou LH, Kim KP (2010) Mass spectrometry based cellular phosphoinositides profiling and phospholipid analysis: a brief review. *Exp Mol Med* 42: 1–11. 10.3858/em.2010.42.1.001 [doi].
- Fuchs B, Suss R, Schiller J (2011) An update of MALDI-TOF mass spectrometry in lipid research. *Prog Lipid Res* 50: 132. S0163-7827(10)00049-4 [pii];10.1016/j.plipres.2010.10.001 [doi].
- Ferreira CR, Saraiva SA, Catharino RR, Garcia JS, Gozzo FC, et al. (2010) Single embryo and oocyte lipid fingerprinting by mass spectrometry. *J Lipid Res* 51: 1218–1227. jlr.D001768 [pii];10.1194/jlr.D001768 [doi].
- Apparicio M, Ferreira CR, Tata A, Santos VG, Alves AE, et al. (2012) Chemical composition of lipids present in cat and dog oocyte by matrix-assisted desorption ionization mass spectrometry (M. *Reprod Domest Anim* 47 Suppl 6: 113–117. 10.1111/rda.12003 [doi].
- Ferreira CR, Pirro V, Eberlin LS, Hallett JE, Cooks RG (2012) Developmental phases of individual mouse preimplantation embryos characterized by lipid signatures using desorption electrospray ionization mass spectrometry. *Anal Bioanal Chem* 404: 2915–2926. 10.1007/s00216-012-6426-4 [doi].
- Tata A, Sudano MJ, Santos VG, Landim-Alvarenga FD, Ferreira CR, et al. (2013) Optimal single-embryo mass spectrometry fingerprinting. *J Mass Spectrom* 48: 844–849. 10.1002/jms.3231 [doi].
- Raychaudhuri S, Stuart JM, Altman RB (2000) Principal components analysis to summarize microarray experiments: application to sporulation time series. *Pac Symp Biocomput* 455–466.
- Eisen MB, Spellman PT, Brown PO, Botstein D (1998) Cluster analysis and display of genome-wide expression patterns. *Proc Natl Acad Sci U S A* 95: 14863–14868.
- Sturmev RG, Reis A, Leese HJ, McEvoy TG (2009) Role of fatty acids in energy provision during oocyte maturation and early embryo development. *Reprod*

- Domest Anim 44 Suppl 3: 50–58. RDA1402 [pii];10.1111/j.1439-0531.2009.01402.x [doi].
19. Loewenstein JE, Cohen AI (1964) Dry mass, lipid content and protein content of the intact and zona-free mouse ovum. *J Embryol Exp Morphol* 12: 113–121.
 20. Kolesnick RN, Goni FM, Alonso A (2000) Compartmentalization of ceramide signaling: Physical foundations and biological effects. *Journal of Cellular Physiology* 184: 285–300.
 21. Kolesnick R (2002) The therapeutic potential of modulating the ceramide/sphingomyelin pathway. *Journal of Clinical Investigation* 110: 3–8.
 22. Hannun YA, Obeid LM (2002) The ceramide-centric universe of lipid-mediated cell regulation: Stress encounters of the lipid kind. *Journal of Biological Chemistry* 277: 25847–25850.
 23. Morita Y, Perez GI, Paris F, Miranda SR, Ehleiter D, et al. (2000) Oocyte apoptosis is suppressed by disruption of the acid sphingomyelinase gene or by sphingosine-1-phosphate therapy. *Nat Med* 6: 1109–1114. 10.1038/80442 [doi].
 24. Perez GI, Jurisicova A, Matikainen T, Moriyama T, Kim MR, et al. (2005) A central role for ceramide in the age-related acceleration of apoptosis in the female germline. *FASEB J* 19: 860–862. 04-2903fje [pii];10.1096/fj.04-2903fje [doi].
 25. Riggs R, Mayer J, Dowling-Lacey D, Chi TF, Jones E, et al. (2010) Does storage time influence postthaw survival and pregnancy outcome? An analysis of 11,768 cryopreserved human embryos. *Fertil Steril* 93: 109–115. S0015-0282(08)04122-8 [pii];10.1016/j.fertnstert.2008.09.084 [doi].
 26. Yan J, Suzuki J, Yu XM, Qiao J, Kan FW, et al. (2011) Effects of duration of cryo-storage of mouse oocytes on cryo-survival, fertilization and embryonic development following vitrification. *J Assist Reprod Genet* 28: 643–649. 10.1007/s10815-011-9563-3 [doi].
 27. Monzo C, Haouzi D, Roman K, Assou S, Dechaud H, et al. (2012) Slow freezing and vitrification differentially modify the gene expression profile of human metaphase II oocytes. *Hum Reprod* 27: 2160–2168. des153 [pii];10.1093/humrep/des153 [doi].
 28. Katz-Jaffe MG, Larman MG, Sheehan CB, Gardner DK (2008) Exposure of mouse oocytes to 1,2-propanediol during slow freezing alters the proteome. *Fertil Steril* 89: 1441–1447. S0015-0282(07)01006-0 [pii];10.1016/j.fertnstert.2007.03.098 [doi].
 29. Kang HS, Lee SC, Park YS, Jeon YE, Lee JH, et al. (2011) Protein and lipid MALDI profiles classify breast cancers according to the intrinsic subtype. *BMC Cancer* 11: 465. 1471-2407-11-465 [pii];10.1186/1471-2407-11-465 [doi].
 30. Kang S, Lee A, Park YS, Lee SC, Park SY, et al. (2011) Alteration in lipid and protein profiles of ovarian cancer: similarity to breast cancer. *Int J Gynecol Cancer* 21: 1566–1572. 10.1097/IGC.0b013e318226c5f5 [doi];00009577-201112000-00011 [pii].
 31. Lee GK, Lee HS, Park YS, Lee JH, Lee SC, et al. (2012) Lipid MALDI profile classifies non-small cell lung cancers according to the histologic type. *Lung Cancer* 76: 197–203. S0169-5002(11)00531-9 [pii];10.1016/j.lungcan.2011.10.016 [doi].
 32. Sudano MJ, Santos VG, Tata A, Ferreira CR, Paschoal DM, et al. (2012) Phosphatidylcholine and sphingomyelin profiles vary in *Bos taurus indicus* and *Bos taurus taurus* in vitro- and in vivo-produced blastocysts. *Biol Reprod* 87: 130. biolreprod.112.102897 [pii];10.1095/biolreprod.112.102897 [doi].
 33. Ferreira CR, Eberlin LS, Hallett JE, Cooks RG (2012) Single oocyte and single embryo lipid analysis by desorption electrospray ionization mass spectrometry. *Journal of Mass Spectrometry* 47: 29–33.
 34. Cha SK, Kim BY, Kim MK, Kim YS, Lee WS, et al. (2011) Effects of various combinations of cryoprotectants and cooling speed on the survival and further development of mouse oocytes after vitrification. *Clin Exp Reprod Med* 38: 24–30. 10.5653/cepm.2011.38.1.24 [doi].
 35. Gomes CM, Silva CA, Acevedo N, Baracat E, Serafini P, et al. (2008) Influence of vitrification on mouse metaphase II oocyte spindle dynamics and chromatin alignment. *Fertil Steril* 90: 1396–1404. S0015-0282(07)03168-8 [pii];10.1016/j.fertnstert.2007.08.025 [doi].
 36. Bang S, Shin H, Song H, Suh CS, Lim HJ (2014) Autophagic activation in vitrified-warmed mouse oocytes. *Reproduction* 148: 11–19. REP-14-0036 [pii];10.1530/REP-14-0036 [doi].
 37. Spangenburg EE, Pratt SJ, Wohlers LM, Lovering RM (2011) Use of BODIPY (493/503) to visualize intramuscular lipid droplets in skeletal muscle. *J Biomed Biotechnol* 2011: 598358. 10.1155/2011/598358 [doi].
 38. Castaneda CA, Kaye P, Pantaleon M, Phillips N, Norman S, et al. (2013) Lipid content, active mitochondria and brilliant cresyl blue staining in bovine oocytes. *Theriogenology* 79: 417–422. S0093-691X(12)00569-9 [pii];10.1016/j.theriogenology.2012.10.006 [doi].
 39. Bligh EG, Dyer WJ (1959) A rapid method of total lipid extraction and purification. *Can J Biochem Physiol* 37: 911–917.
 40. Shanta SR, Zhou LH, Park YS, Kim YH, Kim Y, et al. (2011) Binary matrix for MALDI imaging mass spectrometry of phospholipids in both ion modes. *Anal Chem* 83: 1252–1259. 10.1021/ac1029659 [doi].
 41. Park YS, Yoo CW, Lee SC, Park SJ, Oh JH, et al. (2011) Lipid profiles for intrahepatic cholangiocarcinoma identified using matrix-assisted laser desorption/ionization mass spectrometry. *Clin Chim Acta* 412: 1978–1982. S0009-8981(11)00385-8 [pii];10.1016/j.cca.2011.07.008 [doi].
 42. Edwards JL, Kennedy RT (2005) Metabolomic analysis of eukaryotic tissue and prokaryotes using negative mode MALDI time-of-flight mass spectrometry. *Anal Chem* 77: 2201–2209. 10.1021/ac048323r [doi].
 43. Suckau D, Resemann A, Schuerenberg M, Hufnagel P, Franzen J, et al. (2003) A novel MALDI LIFT-TOF/TOF mass spectrometer for proteomics. *Analytical and Bioanalytical Chemistry* 376: 952–965.
 44. Gibb S, Strimmer K (2012) MALDIquant: a versatile R package for the analysis of mass spectrometry data. *Bioinformatics* 28: 2270–2271. bts447 [pii];10.1093/bioinformatics/bts447 [doi].
 45. Xia J, Wishart DS (2011) Web-based inference of biological patterns, functions and pathways from metabolomic data using MetaboAnalyst. *Nat Protoc* 6: 743–760. nprot.2011.319 [pii];10.1038/nprot.2011.319 [doi].